

The Gas-Phase Reaction of Silylene with Acetaldehyde. 2. Theoretical Calculations of Isotope Effects for SiH₂ versus SiD₂ Addition

Rosa Becerra

Instituto de Química-Física "Rocasolano", C.S.I.C., C/Serrano 119, 28006 Madrid, Spain

J. Pat Cannady

Dow Corning Corporation, P.O. Box 995, Mail 128, Midland, Michigan 48686-0995

Robin Walsh*

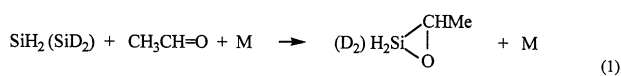
Department of Chemistry, University of Reading, Whiteknights, P.O. Box 224, Reading RG6 6AD, U.K.

Received: April 30, 2002; In Final Form: August 22, 2002

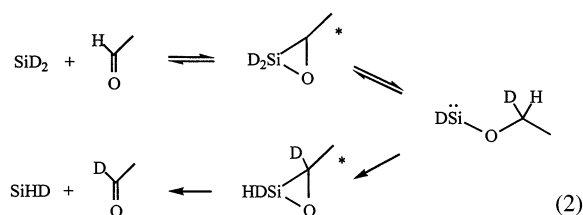
Calculations of isotope effects for the gas-phase reaction of silylene with acetaldehyde have been carried out using a combination of ab initio, transition state, and RRKM theories. Ab initio calculations were used to provide optimized structures at the HF/6-31G(d) level along the reaction coordinate at fixed Si···O distances. These structures were matched to previously measured reaction *A* factors (via entropies of activation), to find the transition state structures (geometries and vibrational wavenumbers) appropriate to each temperature at which previous rate constant measurements were made. Transition state calculations were then made to obtain the isotope effect $k_{1,H}/k_{1,D}$ for the bimolecular addition process. RRKM calculations were then undertaken which gave the isotope effect pressure dependence, at the pressures of the experimental study. The calculated overall isotope effects, k_H/k_D , which were only slightly temperature and pressure dependent, lay in the range 1.005–1.252. These are in good agreement with experimental values. Uncertainties arising from reactant orientation are discussed. The reason for the small isotope effects arises from a compensation of contributing factors due to the looseness of the transition state.

Introduction

In part 1 of this study,¹ experimental measurements of the rate constants of addition of SiH₂ and SiD₂ to CH₃CHO over a range of temperatures and pressures have been reported together with ab initio calculations of the underlying reaction potential energy surface. The results obtained have shown that the kinetic isotope effects k_D/k_H are close to unity and not subject to large variations with temperature and pressure. The rate constants themselves, however, are pressure dependent, and RRKM modeling shows them to be consistent with an association mechanism, viz.,



The ab initio calculations support this mechanism but also indicate, inter alia, that the process occurs via the initial formation of a silacarbonyl ylid, which, in addition to giving 3-methylsiloxirane through ring closure, can also rearrange to form siloxyethene via a 1,4 H-shift process and ethoxysilylene via a 1,3 H-shift process. The absence of a large isotope effect of the kind observed in other silylene addition reactions^{2–5} indicates that the potential isotopic scrambling process



is not occurring. This lack of effect, in contrast to the other systems,^{2–5} can be attributed to the extra stabilization of the silylene product by the ethoxy group. The ab initio calculations are in agreement with this conclusion. What remains to be shown, however, is whether an appropriate transition state model for reaction 1 can reproduce the observed isotope effects. The transition state requirements for this type of calculation are more demanding than those for testing the pressure dependence alone (as undertaken previously¹). This paper therefore describes first some further ab initio calculations designed to specify the transition state structure and vibrations, second the transition state theoretical (TST) calculations themselves of the rate constants and isotope effects at the second-order limit, and third the calculation of the pressure dependence of the isotope effect. There have been no previous calculations of this type on the reaction systems described here.

Theory

Ab Initio Calculations. The electronic structure calculations were performed with the Gaussian 94 software package⁶ as described previously.¹ Stationary point structures were determined by energy minimization at the MP2=Full/6-31G(d) level.⁷ Transition state structures were characterized as first-order saddle points by calculation of the Hessian matrix. Stable structures, corresponding to energy minima, were identified as possessing no negative eigenvalues of the Hessian, while transition states were identified as having one and only one negative eigenvalue. For nonstationary points (see below) calculations were carried out only to the HF/6-31G(d) level of theory. For the purposes of this exercise, this level of calculation was sufficient to yield reliable geometries and vibrational

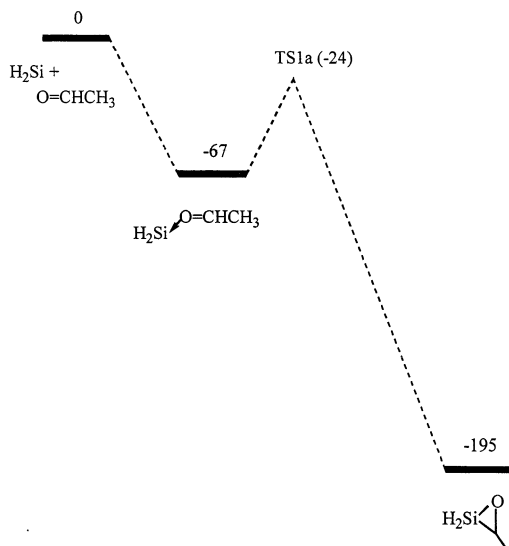


Figure 1. Partial potential surface for SiH_2 (SiD_2) addition to acetaldehyde. Enthalpies (kJ mol^{-1}) calculated at ab initio G2 level (ref 1).

wavenumbers, although the latter were corrected by the 0.893 factor, acknowledged as appropriate for this level.⁸

The part of the surface appropriate to this study is that leading from reactants to 3-methylsiloxirane. The PE surface for this, determined previously at the higher G2 level, is shown in Figure 1. This shows the three stationary points corresponding to the adduct, viz. the silacarbonyl ylid, the transition state, TS1a, and 3-methylsiloxirane, the final product of concern. We have shown in part 1¹ that further reactions of 3-methylsiloxirane are not significant for rate determining purposes although small contributions from side reactions of the adduct may have a minor effect on the rate. For the purposes of the TST calculations, the important thing is to locate the transition state for the reaction. It was apparent from part 1 that the real transition state had a far looser structure than that of TS1a. Thus TS1a is not rate determining and the effective bottleneck for reaction is occurring during the initial encounter of SiH_2 with MeCHO . Unfortunately, there is no ab initio determined stationary point in this region, corresponding to a fixed activated complex geometry. In principle this kind of a problem can be addressed by flexible transition state theory (FTST).^{9–11} However this would require a realistic representation of the angular as well as linear approach potentials of the two reacting species, which was not within our calculational compass. Instead a more empirical kinetic/transition state theoretical criterion was employed. The following approach was adopted.

(a) The geometries and vibration (harmonic) wavenumbers for a series of $\text{SiH}_2 \cdots \text{CH}_3\text{CHO}$ structures at different (frozen) $\text{Si} \cdots \text{O}$ separations were determined. This was done for both SiH_2 and SiD_2 adducts.

(b) For the SiH_2 adducts these quantities were used, in conjunction with those of 3-methylsiloxirane, to calculate activation entropies ΔS^\ddagger and thereby a series of A factors (via $A = (\text{Le}kT/h)e^{\Delta S^\ddagger/R}$)⁹ for the decomposition of 3-methylsiloxirane (i.e., the reverse reaction to that of the present study).

(c) These “theoretical” A factors were then compared with those obtained previously¹ from the experimental kinetics and overall thermodynamics (ΔS° for 3-methylsiloxirane formation). By a process of interpolation it was then possible to find the best structure, energy minimized, at a specific $\text{Si} \cdots \text{O}$ bond distance corresponding to the experimental A factor estimate. Because of the variation of A factor with temperature, previously

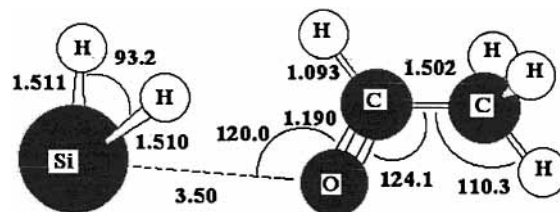


Figure 2. Ab initio MP2=Full/6-31G(d) calculated structure of activated complex species at 398 K with constrained $\text{Si} \cdots \text{O}$ distance for reaction of $\text{SiH}_2 + \text{CH}_3\text{CHO}$ (*anti-in* structure). Distances are given in angstroms and angles in degrees. The zwitterionic nature of this complex is indicated by the calculated partial charges, viz. +0.28 (Si), -0.52 (O), +0.37 (C of $\text{C}=\text{O}$), -0.60 (C of CH_3).

TABLE 1: A Factors for 3-Methylsiloxirane Decomposition¹ Used for TST Fitting of ab Initio Structures, and the Derived $\text{Si} \cdots \text{O}$ Bond Distances

T/K	$\log(A/\text{s}^{-1})$	$r_{\text{Si} \cdots \text{O}}/\text{\AA}$
296	17.81	3.75
339	17.74	3.63
398	17.65	3.51
477	17.52	3.37
597	17.29	3.19

TABLE 2: Ab Initio (HF/6-31G(d)) Structure and Vibrations^a for the Transition State at 296 K for SiH_2 (and SiD_2) + MeCHO : $r_{\text{Si} \cdots \text{O}} = 3.75 \text{ \AA}$

parameter ^b	Structure	
	TS,H	TS,D
I^+	12085	13927
C–H str (4)	2967, 2913, 2864 2830	2967, 2913, 2864 2830
Si–H str (2)	1975, 1962	1419, 1413
CH_3 def (3)	1442, 1433, 1372	1442, 1433, 1372
C–H def (2)	1399, 1131	1399, 1131
CH_3 rock (2)	1102, 767	1102, 767
SiH_2 def	1011	728
$\text{C}=\text{O}$ str	1806	1806
C–C str	863	863
$\text{Si} \cdots \text{O}$ str	imaginary	imaginary
SiH_2 wag, rock	233, 180	170, 125
C–C–O bend	490	490
$\text{C}=\text{O} \cdots \text{Si}$ bend	32	31
$\text{C}=\text{O}$ twist	30	30
$\text{Si} \cdots \text{O}$ twist	17	15
CH_3 int rot	135	139
ZPE ^c	14477	13725

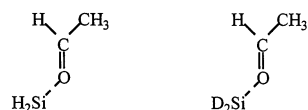
^a Wavenumbers adjusted by $\times 0.893$.⁸ ^b Units: moment of inertia ($\text{u}\text{\AA}^2$)^{3/2}, wavenumbers and ZPE, cm^{-1} . ^c Zero-point energy.

noted,¹ this had to be done at each temperature of study. The experimental A factors from the previous study and the $\text{Si} \cdots \text{O}$ bond distances corresponding to the activated complex structures which fit them are shown in Table 1.

(d) Once these structures had been identified, the ab initio calculations automatically provided the necessary transition state parameters for their SiD_2 counterparts.

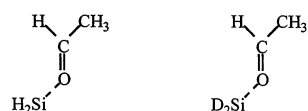
The general structure of the complex (one example) is shown in Figure 2. The structural parameters and wavenumbers of the transition state species are shown in Tables 2–6. Those for 3-methylsiloxirane and 3-methylsiloxirane-1- d_2 are shown in Table 7.

The lack of a TS maximum on the PE surface means that the IRC criterion of quantum-chemical calculations is not straightforward to apply here. Nevertheless it is clear that the main geometrical parameter to the reaction coordinate must be

TABLE 3: Ab Initio (HF/6-31G(d)) Structure and Vibrations^a for the Transition State at 339 K for SiH₂ (and SiD₂) + MeCHO: $r_{\text{Si}\cdots\text{O}} = 3.63 \text{ \AA}$ 

parameter ^b	TS,H	TS,D
I ⁺	11558	13314
C–H str (4)	2967, 2913, 2864 2832	2967, 2913, 2864 2832
Si–H str (2)	1974, 1960	1419, 1412
CH ₃ def (3)	1442, 1433, 1372	1442, 1433, 1372
C–H def (2)	1399, 1131	1399, 1131
CH ₃ rock (2)	1102, 767	1102, 767
SiH ₂ def	1011	728
C=O str	1805	1805
C–C str	863	863
Si–O str	imaginary	imaginary
SiH ₂ wag, rock	253, 196	185, 138
C–C–O bend	490	490
C=O \cdots Si bend	36	35
C=O twist	32	32
Si \cdots O twist	18	17
CH ₃ int rot	135	136
ZPE ^c	14498	13741

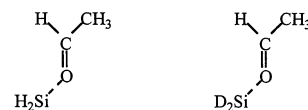
^a Wavenumbers adjusted by $\times 0.893$.⁸ ^b Units: moment of inertia ($\text{u}\text{\AA}^2$)^{3/2}, wavenumbers and ZPE, cm^{-1} . ^c Zero-point energy.

TABLE 4: Ab Initio (HF/6-31G(d)) Structure and Vibrations^a for the Transition State at 398 K for SiH₂ (and SiD₂) + MeCHO: $r_{\text{Si}\cdots\text{O}} = 3.51 \text{ \AA}$ 

parameter ^b	TS,H	TS,D
I ⁺	11006	12670
C–H str (4)	2968, 2914, 2865 2835	2968, 2914, 2865 2835
Si–H str (2)	1973, 1958	1418, 1410
CH ₃ def (3)	1442, 1433, 1372	1442, 1433, 1372
C–H def (2)	1400, 1131	1400, 1131
CH ₃ rock (2)	1102, 768	1102, 768
SiH ₂ def	1011	728
C=O str	1804	1804
C–C str	864	864
Si–O str	imaginary	imaginary
SiH ₂ wag, rock	274, 213	201, 155
C–C–O bend	491	490
C=O \cdots Si bend	41	40
C=O twist	36	36
Si \cdots O twist	19	18
CH ₃ int rot	135	133
ZPE ^c	14525	13764

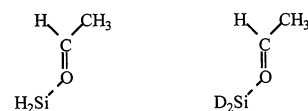
^a Wavenumbers adjusted by $\times 0.893$.⁸ ^b Units: moment of inertia ($\text{u}\text{\AA}^2$)^{3/2}, wavenumbers and ZPE, cm^{-1} . ^c Zero-point energy.

the Si \cdots O distance. However, it is possible to envisage several approach orientations of the reacting species. Therefore, in addition to the calculations described above, we carried out another set of calculations involving three other possible approach geometries of the reactant species for the particular case of the Si \cdots O distance of 3.5 Å, corresponding to the TS structure at the median temperature of 398 K. These gave the structures shown in Figure 3. They correspond first to *anti*- and *syn*-positions of the SiH₂ with respect to the CH₃ group in the CH₃CHO fragment. Second “*in*” and “*out*” refer to the orientation of the H₂ in the SiH₂ moiety, pointing either toward or

TABLE 5: Ab Initio (HF/6-31G(d)) Structure and Vibrations^a for the Transition State at 477 K for SiH₂ (and SiD₂) + MeCHO: $r_{\text{Si}\cdots\text{O}} = 3.37 \text{ \AA}$ 

parameter ^b	TS,H	TS,D
I ⁺	10427	12028
C–H str (4)	2969, 2914, 2866 2838	2969, 2914, 2866 2838
Si–H str (2)	1971, 1956	1417, 1408
CH ₃ def (3)	1442, 1433, 1372	1442, 1433, 1372
C–H def (2)	1400, 1132	1400, 1132
CH ₃ rock (2)	1103, 769	1103, 769
SiH ₂ def	1010	727
C=O str	1802	1802
C–C str	865	865
Si–O str	imaginary	imaginary
SiH ₂ wag, rock	301, 234	219, 170
C–C–O bend	492	491
C=O \cdots Si bend	48	47
C=O twist	40	40
Si \cdots O twist	20	20
CH ₃ int rot	135	134
ZPE ^c	14556	13789

^a Wavenumbers adjusted by $\times 0.893$.⁸ ^b Units: moment of inertia ($\text{u}\text{\AA}^2$)^{3/2}, wavenumbers and ZPE, cm^{-1} . ^c Zero-point energy.

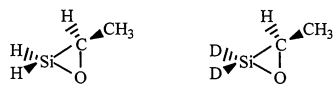
TABLE 6: Ab Initio (HF/6-31G(d)) Structure and Vibrations^a for the Transition State at 597 K for SiH₂ (and SiD₂) + MeCHO: $r_{\text{Si}\cdots\text{O}} = 3.19 \text{ \AA}$ 

parameter ^b	TS,H	TS,D
I ⁺	9644	11148
C–H str (4)	2969, 2914, 2866 2843	2969, 2914, 2866 2843
Si–H str (2)	1969, 1953	1415, 1406
CH ₃ def (3)	1442, 1433, 1372	1442, 1433, 1372
C–H def (2)	1400, 1132	1400, 1132
CH ₃ rock (2)	1103, 769	1103, 769
SiH ₂ def	1010	727
C=O str	1800	1800
C–C str	865	865
Si–O str	imaginary	imaginary
SiH ₂ wag, rock	341, 271	250, 195
C–C–O bend	493	492
C=O \cdots Si bend	58	57
C=O twist	46	46
Si \cdots O twist	20.5	20.5
CH ₃ int rot	135	134
ZPE ^c	14602	13825

^a Wavenumbers adjusted by $\times 0.893$.⁸ ^b Units: moment of inertia ($\text{u}\text{\AA}^2$)^{3/2}, wavenumbers and ZPE, cm^{-1} . ^c Zero-point energy.

away from the CH₃CHO fragment. The calculations show that with each of the four starting configurations (*anti-in*, *syn-in*, *anti-out*, and *syn-out*) a different minimum energy structure (and minimum energy value) is obtained although the only constraint is the Si \cdots O fixed distance. Although the *anti-in* structure is energetically the lowest, the energy differences are very small. This shows that each of the differently oriented configurations represents a potential pathway.

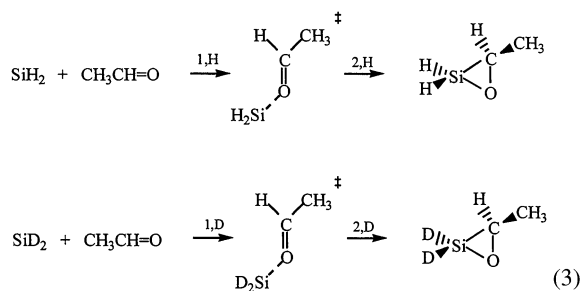
In the next section the systematic isotope effect calculations have been carried out using the most stable *anti-in* configuration. However we have also investigated the isotope effects for the other configurations at the single Si \cdots O distance of 3.5 Å.

TABLE 7: Ab Initio (HF/6-31G(d)) Structure and Vibrations^a for 3-Methylsiloxirane and 3-Methylsiloxirane-1-d₂


parameter ^b	mol,H	mol,D
I ⁺	4886	5494
C-H str (4)	2942, 2920, 2912 2858	2942, 2920, 2912 2858
Si-H str (2)	2174, 2172	1574, 1555
CH ₃ def (3)	1467, 1452, 1397	1467, 1452, 1397
C-H def (2)	1331, 1164	1330, 1162
CH ₃ rock (2)	1062, 974	1056, 964
SiH ₂ def, wag, rock, twist	948, 776, 640, 523	705, 520, 495, 440
C-O str	693	684
C-C str	1089	1088
Si-O str	871	874
C-Si str	603	656
SiH ₂ wag, rock	341, 271	250, 195
C-C-O bend	335	320
C-C-Si bend	239	220
CH ₃ int rot	203	202
ZPE ^c	15873	14897

^a Wavenumbers adjusted by $\times 0.893$.⁸ ^b Units: moment of inertia ($\text{u}\text{\AA}^2$)^{3/2}, wavenumbers and ZPE, cm^{-1} . ^c Zero-point energy.

Transition State Theory Calculations. For a pair of isotopically related reactions such as those investigated here, viz.:



Transition state theory¹² gives the expression

$$\frac{k_{1,\text{H}}}{k_{1,\text{D}}} = \frac{q_{\text{TS,H}}^\ddagger}{q_{\text{TS,D}}^\ddagger} \frac{q_{\text{SiD}_2}}{q_{\text{SiH}_2}} e^{-(\Delta E^\ddagger(\text{H}) - \Delta E^\ddagger(\text{D}))/kT} \quad (\text{X})$$

where $q_{\text{TS,H}}^\ddagger$ and $q_{\text{TS,D}}^\ddagger$ refer to the activated complex partition functions corrected for reaction coordinate motion; q_{SiD_2} and q_{SiH_2} refer to the reactant partition functions, and $\Delta E^\ddagger(\text{H})$ and $\Delta E^\ddagger(\text{D})$ are the zero-point energy differences between activated complexes and reactants. Partition function ratios were calculated using the standard formulas for translation (particle in a box), rotation (rigid rotor), and vibration (harmonic oscillator).¹² The use of ratios allows considerable simplification of the calculations. The details of the calculations for each ratio and terms are as follows.

(a) $q_{\text{SiD}_2}/q_{\text{SiH}_2}$. Moment of inertia values and vibrational wavenumbers for SiH₂ and SiD₂ were taken from the theoretical calculations (for consistency) although experimental values for these quantities exist. This makes a negligible difference. The values of the individual contributions (at each temperature) are shown in Table 8.

(b) $q_{\text{TS,H}}^\ddagger/q_{\text{TS,D}}^\ddagger$. The data required for these calculations are all shown in Tables 2–6. The values of the individual contributions (at each temperature) are shown in Table 9. The nonmonotonic changes with temperature in the vibrational

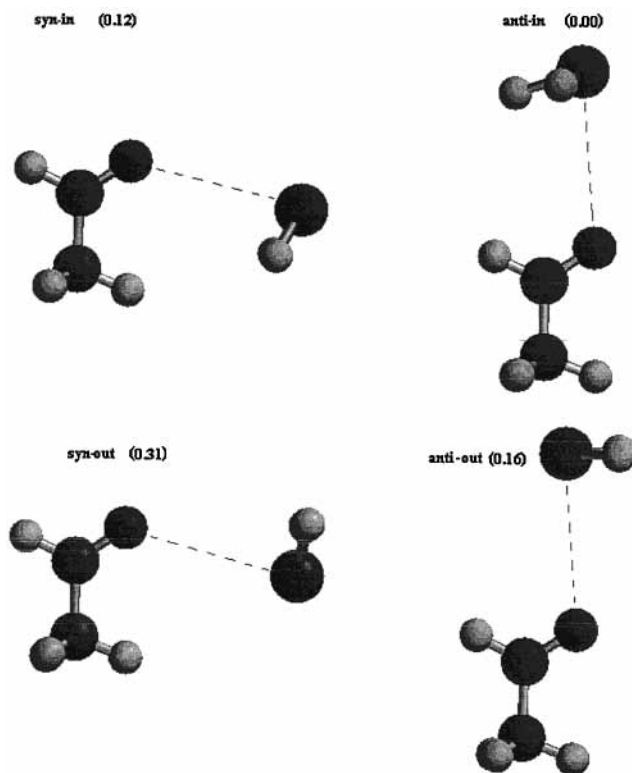


Figure 3. Ab initio (HF/6-31G(d)) calculated structures of activated complex species with constrained Si \cdots O distance of 3.5 Å for different approach geometries of SiH₂ and CH₃CHO. Figures in parentheses are relative energies in kJ mol^{-1} .

TABLE 8: Contributions to $q_{\text{SiD}_2}/q_{\text{SiH}_2}$ at Different Temperatures

T/K	trans	rot ^a	vib ^b	total
296	1.102	2.70	1.025	3.05
339	1.102	2.70	1.038	3.09
398	1.102	2.70	1.060	3.15
477	1.102	2.70	1.096	3.26
597	1.102	2.70	1.159	3.45

^a Moment of inertia/ $\text{u}\text{\AA}^2$: SiH₂: 7.18, 8.66, 15.85; SiD₂: 13.45, 17.32, 30.77. ^b Vibrational wavenumbers/ cm^{-1} : SiH₂: 1984, 1974, 1009; SiD₂: 1425, 1422, 726.

TABLE 9: Contributions to $q_{\text{TS,H}}^\ddagger/q_{\text{TS,D}}^\ddagger$ at Different Temperatures

T/K	$r_{\text{Si}\cdots\text{O}}$	trans	rot	vib	total
296	3.75	0.961	0.868	0.564	0.470
339	3.63	0.961	0.869	0.568	0.474
398	3.51	0.961	0.869	0.551	0.460
477	3.37	0.961	0.867	0.570	0.474
597	3.19	0.961	0.866	0.529	0.440

contributions arose from the variety of temperature dependences of different modes, in particular the different “switch-on” points of the stretching modes of Si–H and Si–D in the complex.

(c) $\exp[-(\Delta E^\ddagger(\text{H}) - \Delta E^\ddagger(\text{D}))/kT]$. The data required for these calculations are all shown in Tables 2–6. The values of the zero-point energies differences and resulting contributions are shown in Table 10.

(d) $k_{1,\text{H}}/k_{1,\text{D}}$. The final values collected from each term in Tables 8–10 are shown in Table 11. These correspond to the high-pressure limit (infinite pressure) value for the isotope effect for the most stable (*anti-in*) structure. The calculations for the other structures at Si \cdots O = 3.5 Å were very similar to those described, and therefore the details are not shown. However the outcome was values for $k_{1,\text{H}}/k_{1,\text{D}}$ of 1.037 (*syn-in*), 0.977

TABLE 10: Zero-Point Energy Contributions^a at Different Temperatures

<i>T</i> /K	$\Delta E^\ddagger(\text{H})^b$	$\Delta E^\ddagger(\text{D})^c$	$\Delta E^\ddagger(\text{H}) - \Delta E^\ddagger(\text{D})$	$\exp[-(\Delta\Delta E^\ddagger)/bT]^d$
296	11994	11939	55	0.765
339	12015	11955	60	0.775
398	12042	11978	64	0.793
477	12073	12003	70	0.810
597	12119	12039	80	0.824

^a ΔE values all in cm^{-1} . ^b $\Delta E^\ddagger(\text{H}) = E_{\text{TS,H}}^\ddagger - E_{\text{SiH}_2}$. ^c $\Delta E^\ddagger(\text{D}) = E_{\text{TS,D}}^\ddagger - E_{\text{SiD}_2}$. ^d $b = k/hc$.

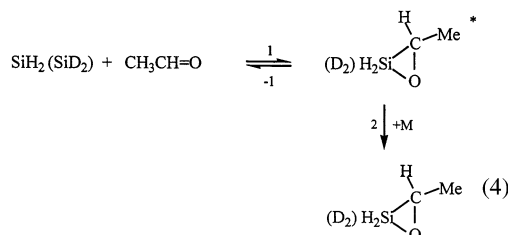
TABLE 11: Contributions to TST Kinetic Isotope Effect from Each Term (Equation X)

<i>T</i> /K	$q_{\text{SiD}_2}/q_{\text{SiH}_2}$	$q_{\text{TS,H}}^\ddagger/q_{\text{TS,D}}^\ddagger$	$\exp[-(\Delta\Delta E^\ddagger)/bT]$	$k_{1,\text{H}}/k_{1,\text{D}}$
296	3.05	0.470	0.765	1.097
339	3.09	0.474	0.775	1.135
398	3.15	0.460	0.793	1.149
477	3.26	0.474	0.810	1.252
597	3.45	0.440	0.824	1.251

(*anti-out*) and 0.994 (*syn-out*) compared with 1.149 for *anti-in* shown in Table 11. This shows the variation of the isotope effect with possible orientation of approach of the reacting species.

Since the association reaction is pressure dependent, $k_{1,\text{H}}/k_{1,\text{D}}$ values need to be corrected. The correction factors for this were calculated by RRKM theory,^{9,13} details of which are described in the next section.

RRKM Calculations. The pressure dependence of an association reaction corresponds exactly to that of the reverse unimolecular dissociation process and therefore so does the kinetic isotope effect of the pressure dependence. If the reaction is treated as a simple reverse Lindemann mechanism, viz.



then the isotope effect is given by

$$\frac{k_{\text{H}}}{k_{\text{D}}} = \frac{k_{1,\text{H}}(1 + k_{-1,\text{D}}/k_2[\text{M}])}{k_{1,\text{D}}(1 + k_{-1,\text{H}}/k_2[\text{M}])} \quad (\text{Y})$$

The RRKM expression corresponding to eq Y is considerably more complex^{9,13} and is not given in full here, but the expression may be written in simplified form as

$$\frac{k_{\text{H}}}{k_{\text{D}}} = \frac{k_{1,\text{H}}}{k_{1,\text{D}}} f$$

where f is the isotopic factor, calculated by RRKM, corresponding to the pressure dependence. Since $k_{1,\text{H}}/k_{1,\text{D}}$ corresponds to the TST calculated (infinite pressure) isotope effect, the factor f can be calculated as the ratio of “falloff” effects in the decompositions of 3-methylsiloxirane-1-*d*₂ and 3-methylsiloxirane itself. We have already carried out RRKM calculations for this reaction in part 1, to fit the observed pressure dependence.¹ The exercise here is thus a simple repeat of these calculations, using the more refined activation complexes obtained by the ab initio calculations. Because the complexes were constrained to fit the decomposition A factors (at each

TABLE 12: RRKM Calculated Degrees of Falloff (k/k^∞) for 3-Methylsiloxirane and 3-Methylsiloxirane-1-*d*₂ and Calculated Pressure Dependent Isotope Effects (f)

<i>P</i> /Torr	$k_{\text{H}}/k_{\text{H}}^\infty$	$k_{\text{D}}/k_{\text{D}}^\infty$	f
<i>T</i> = 296 K			
100	0.977	0.984	0.993
30	0.942	0.957	0.984
10	0.879	0.906	0.971
3	0.769	0.813	0.946
1	0.631	0.689	0.916
<i>T</i> = 339 K			
100	0.959	0.971	0.989
30	0.908	0.929	0.977
10	0.824	0.859	0.959
3	0.690	0.743	0.929
1	0.542	0.605	0.895
<i>T</i> = 398 K			
100	0.920	0.938	0.982
30	0.838	0.867	0.966
10	0.726	0.767	0.946
3	0.571	0.624	0.916
1	0.423	0.478	0.885
<i>T</i> = 477 K			
100	0.834	0.865	0.964
30	0.710	0.753	0.942
10	0.570	0.624	0.914
3	0.411	0.467	0.881
1	0.280	0.330	0.847
<i>T</i> = 597 K			
100	0.640	0.678	0.944
30	0.482	0.526	0.916
10	0.344	0.385	0.891
3	0.217	0.252	0.861
1	0.132	0.158	0.834

temperature), the necessary looseness of structure is already built in. The critical energy $E_0 = 221.8 \text{ kJ mol}^{-1}$ was used as previously, because this value gave the best fit to the pressure dependence for $\text{SiH}_2 + \text{MeCHO}$. The vibrational and structural parameters required for these calculations have already been given in Tables 2–7. No attempt was made to carry out a sophisticated treatment of adiabatic rotational effects other than to include the moment of inertia ratio I^+/I for each complex at each temperature resulting from the ab initio calculations. This is an approximation, but we do not believe it should lead to serious errors. As previously,¹ we have used a weak collisional (stepladder) model for collisional deactivation with $\langle\Delta E\rangle_{\text{down}} = 12 \text{ kJ mol}^{-1}$ (appropriate to experimental fitting in this system).

The results of our calculations are shown in Table 12. These are expressed in terms of “degree of falloff” k/k^∞ for each system at each temperature and pressure of interest. The desired isotope effect f is therefore the differential degree of falloff ($k_{\text{H}}/k_{\text{H}}^\infty$)/($k_{\text{D}}/k_{\text{D}}^\infty$), which is also shown in the table. The individual degree of falloff $k_{\text{H}}/k_{\text{H}}^\infty$ matches exactly that computed previously,¹ where E_0 was adjusted to fit the observed pressure dependence.

The total isotope effect at each experimental pressure is calculated by combining the TST calculated $k_{1,\text{H}}/k_{1,\text{D}}$ with f . This is shown in Table 13 where it is compared with the experimental results. RRKM calculations of the pressure dependence of the isotope effect for the other possible TS structures of Figure 3 were not carried out. It is known that, provided the thermal A factor of reaction is matched by the TST model, pressure dependence is insensitive to structure. This is the case here for the isotope effect.

Discussion

Ab Initio Calculations. The ab initio structures (*anti-in* species) which provide the basis for the TST and RRKM

TABLE 13: Comparison of Calculated and Experimental Isotope Effects (k_H/k_D) for Reaction of SiH₂ (SiD₂) with Acetaldehyde

P/Torr	k_H/k_D (theory)	k_H/k_D (exptl)
	$T = 296$ K	
∞	1.097	<i>a</i>
100	1.089	0.91 ± 0.14
30	1.079	1.04 ± 0.15
10	1.065	1.02 ± 0.05
3	1.038	0.94 ± 0.13
1	1.005	0.93 ± 0.13
	$T = 339$ K	
∞	1.135	<i>a</i>
100	1.122	1.22 ± 0.18
30	1.109	1.09 ± 0.15
10	1.088	0.94 ± 0.04
3	1.054	0.92 ± 0.13
1	1.016	0.94 ± 0.13
	$T = 398$ K	
∞	1.149	<i>a</i>
100	1.128	0.97 ± 0.14
30	1.110	0.92 ± 0.13
10	1.087	0.88 ± 0.06
3	1.052	0.84 ± 0.12
1	1.017	0.92 ± 0.13
	$T = 477$ K	
∞	1.252	<i>a</i>
100	1.207	1.19 ± 0.17
30	1.179	1.04 ± 0.15
10	1.144	0.88 ± 0.04
3	1.103	1.11 ± 0.16
1	1.060	1.10 ± 0.16
	$T = 597$ K	
∞	1.251	<i>a</i>
100	1.181	1.49 ± 0.20
30	1.146	1.20 ± 0.17
10	1.115	1.06 ± 0.07
3	1.077	0.89 ± 0.13
1	1.043	0.62 ± 0.09

^a Value of 1.0 ± 0.14 was obtained by extrapolation. Error estimate is subjective.

calculations at each temperature do not differ significantly from one another except in the Si \cdots O interatomic distance. The distances in the complexes (3.19–3.75 Å) indicate the considerable bond extension compared with the ylid (2.07 Å) and a normal Si–O bond of ca. 1.63 Å.¹⁴ This shows the looseness of these structures. The SiH₂ (or SiD₂) fragment is very similar in geometry to the free silylene and is bonded with its plane almost perpendicular to the Si \cdots O bond as expected for a species using its empty 3p orbital to form the new bond. The Si \cdots O=C bond angle is close to 120° suggesting the involvement of hybridized O atom orbitals, similar to the situation in van der Waals complexes of carbonyl compounds.¹⁵ Variations of properties with Si \cdots O bond distances (Tables 2–6) are reasonable and expected. The more extended the Si \cdots O, the larger is the species overall moment of inertia [$I^+ = (I_x I_y I_z)^{1/2}$]. The wavenumbers for the SiH₂ (and SiD₂) group wag and rock, the C=O \cdots Si bend and the C=O and Si \cdots O twists all decrease with increasing Si \cdots O distance. The wavenumbers of the other vibrations are largely invariant. Isotopic differences are almost entirely limited to the SiH₂ and SiD₂ group motions.

The important quantities for the purposes of TST calculations are the geometry and vibrational wavenumbers. The HF/6-31G-(d) level used here, together with the adjustment factor for vibrational wavenumbers, are generally regarded as adequate for these quantities, even though higher levels of theory are required to provide good electronic energies. It is generally expected that any deficiencies of structure and vibrational

TABLE 14: Contributions to TST Kinetic Isotope Effect for Three Different Transition State Structures at 296 K

species	$q_{\text{SiD}_2}/q_{\text{SiH}_2}$	$q_{\text{TS,H}}^\ddagger/q_{\text{TS,D}}^\ddagger$	$\exp[-(\Delta\Delta E^\ddagger)/kT]$	$k_{1,H}/k_{1,D}$
TS \cdots encounter ^a	3.05	0.470	0.765	1.097
TS \cdots adduct ^b	3.05	0.585	0.417	0.742
TS1a	3.05	0.608	0.378	0.699

^a *Anti-in* structure. ^b Ylid structure.

properties will be largely canceling between isotopic variants. The effect of the other conformational species (i.e., of the orientation of approach of reactants) is discussed in the next section.

Transition State Theory Calculations. The isotope effects in reaction 1 are secondary in nature and not expected to be large.^{9,12} In this respect the finding of values of $k_{1,H}/k_{1,D}$ in the range 1.10–1.25 (Table 11) is not particularly startling. What is perhaps more interesting are the individual contributions which combine to give this result. These include the significant rotational contribution to $q_{\text{SiD}_2}/q_{\text{SiH}_2}$ of 2.70 (Table 8) and the quite low values of 0.53–0.57 for the vibrational contributions to $q_{\text{TS,H}}^\ddagger/q_{\text{TS,D}}^\ddagger$. It appeared to us somewhat fortuitous that all the partition function and zero-point energy effects almost completely compensate one another. We therefore decided briefly to investigate whether this situation might be more general, as follows. Two further transition states were constructed on the bases of the ab initio calculated geometries and vibrational wavenumbers of the ylid (adduct) and of TS1a (see Figure 2). The same TST exercise was carried out (at 296 K) to obtain the isotope effect $k_{1,H}/k_{1,D}$ for these two species as for the actual transition state at this temperature (TS \cdots encounter = *anti-in*), and the results are compared in Table 14. This table shows that if the transition state had had the somewhat tighter structures of either the ylid or TS1a the isotope effect would have been significantly lower. In fact an inverse effect was found, arising principally from the zero-point energy contribution. Thus on the admittedly limited scope of this exercise it appears that for SiH₂ (SiD₂) addition reactions, significant departures from unity of the kinetic isotope effect may arise depending on the tightness of the transition state. In the present case the looseness of the transition state is established by the high *A* factor for this reaction.

It is hard to estimate uncertainties in the values obtained for $k_{1,H}/k_{1,D}$ in Tables 11 and 14. This is why we also carried out the brief investigation of reactant orientation. This showed clearly that differences in $k_{1,H}/k_{1,D}$ could arise depending on structure (conformation) of the transition state species. For example the isotope effect drops in value by 15% between “*anti-in*” (1.149) and “*anti-out*” (0.977) structures. A Boltzmann factor-weighted mean of the values would give $k_{1,H}/k_{1,D} = 1.035$ some 10% less than the most energetically stable structure. Since the energy differences are very small between the conformational species corresponding to each orientation, this suggests that all approaches will contribute to the reaction flux. Thus these added calculations suggest that the values based on the *anti-in* structure alone may represent an overestimate by up to 10%. While there may be other sources of error in these calculations, these effects probably represent the greatest uncertainty.

A more basic critique of these calculations is that of the model itself. There are two weaknesses. The first is that it is based on the harmonic approximation for vibrations where in fact the weak (transitional) modes bear a close resemblance to hindered rotors. The second is that we have only explored four possible approach geometries, which may be argued as only a limited

fraction of configuration space. There is no doubt that the more realistic approach of FTST^{16–18} with a more detailed PE surface could improve on some of these weaknesses. TST kinetic isotope effect calculations are more forgiving than absolute rate calculations in the sense that some of the possible errors in the approximations will cancel between the corresponding H- and D- species.

RRKM Calculations. These calculations were constrained by (a) the transition state structures required to fit the previously established *A* factors¹ (for 3-methylsiloxirane decomposition) and (b) the *E*₀ value of 221.8 kJ mol⁻¹ required to fit the previously observed pressure dependence. The results obtained (Table 12) show the characteristic inverse (“nonequilibrium”) isotope effect of a unimolecular reaction in its falloff region,⁹ with a progressive decrease in $f(=(k_H/k_H^\infty)/(k_D/k_D^\infty))$ as pressure decreases and temperature increases. It is unlikely that any of the uncertainties in the TST calculations will cause any significant extra effect here. The inclusion of an active rotation, in place of the lowest wavenumber vibration made no difference.

Comparison of Theory and Experiment and General Conclusions. An examination of Table 13 shows reasonable agreement between theory and experiment. The overall theoretical result indicates that the combination of TST and RRKM leads to values that increase with temperature but decrease with pressure such that the overall variation in k_H/k_D is extremely small over the experimental range of conditions. Experimental uncertainties in k_H/k_D are in the range of 4–15% and for most of the experimental values they encompass the theoretical results. Two of the experimental values at 597 K (1.49, 0.62) stand out as probably being in error (as does one at 477 K (0.88)). The *average* of the differences between theory and experiment is +0.10, i.e., the systematic difference is still well within the *average* measurement uncertainty. If the effects of reactant orientation are considered, the decrease in calculated k_H/k_D values would mean that the discrepancies might well drop to almost zero. While our experimental data are too uncertain to make this claim with complete confidence, it is encouraging that a realistic modification of our calculated values moves them in the right direction.

This exercise shows that the measurement of isotope effects in this reaction system is entirely consistent with the mechanism deduced from the kinetic study of SiH₂ alone with CH₃CHO. Although the isotope effect study confirmed the mechanistic conclusions in this case, it is clear from alternative (hypothetical but tighter) structures considered as transition states that significantly different effects would have been arisen in other

cases. Of course, if there had been hidden mechanistic steps which scrambled the isotopic labels, then altogether much larger isotope effects would have arisen such as we found in earlier studies of SiH₂ + C₂H₂ (C₂D₂)^{2–4} and SiH₂ + C₂H₄ (C₂D₄).^{2,3,5} Thus isotopic probing remains a powerful tool for the investigation of the kinetics of silylene reactions.

Acknowledgment. R.B. and R.W. thank Dow-Corning for a grant in support of this work. R.B. also thanks the Spanish DGICYT for support under projects PB98-0537-C02-01 and BQU2000-1163-C01-01.

References and Notes

- (1) Becerra, R.; Cannady, J. P.; Walsh, R. *Phys. Chem. Chem. Phys.* **2001**, *3*, 2343.
- (2) Becerra, R.; Walsh, R. *Kinetics & Mechanisms of Silylene Reactions: A Prototype for Gas-Phase Acid/Base Chemistry*. In *Research in Chemical Kinetics*; Compton, R. G., Hancock, G., Eds.; Elsevier: Amsterdam, 1995; Vol. 3, p 263.
- (3) Jasinski, J. M.; Becerra, R.; Walsh, R. *Chem. Rev.* **1995**, *95*, 1203.
- (4) Becerra, R.; Walsh, R. *Int. J. Chem. Kinet.* **1994**, *26*, 45.
- (5) Al-Rubaiey, N.; Becerra, R.; Walsh, R. *Phys. Chem. Chem. Phys.* **2002**, *4*, 5072.
- (6) Frisch, M. J.; Trucks, G. W.; Schlegel, H. B.; Gill, P. M. W.; Johnson, B. G.; Robb, M. A.; Cheeseman, J. R.; Keith, T.; Petersson, G. A.; Montgomery, J. A.; Raghavachari, K.; Al-Laham, M. A.; Zakrzewski, V. G.; Ortiz, J. V.; Foresman, J. B.; Cioslowski, J.; Stefanov, B. B.; Nanayakkara, A.; Challacombe, M.; Peng, C. Y.; Ayala, P. Y.; Chen, W.; Wong, M. W.; Andres, J. L.; Replogle, E. S.; Gomperts, R.; Martin, R. L.; Fox, D. J.; Binkley, J. S.; Defrees, D. J.; Baker, J.; Stewart, J. P.; Head-Gordon, M.; Gonzales, C.; Pople, J. A. *Gaussian 94*, revision E.2; Gaussian, Inc.: Pittsburgh, 1995.
- (7) MP2=Full: the MP2 calculation is carried out with the inclusion of full correlation of all electrons.
- (8) Pople, J. A.; Scott, A. P.; Wong, M. W.; Radom, L. *Isr. J. Chem.* **1993**, *33*, 345.
- (9) Holbrook, K. A.; Pilling, M. J.; Robertson, S. H. *Unimolecular Reactions*, 2nd ed.; Wiley: Chichester, 1996.
- (10) Wardlaw, D. M.; Marcus, R. A. *J. Phys. Chem.* **1986**, *90*, 5383.
- (11) Truhlar, D. G.; Garrett, B. C.; Klippenstein, S. J. *J. Phys. Chem.* **1996**, *100*, 12771.
- (12) Smith, I. W. M. *Kinetics and Dynamics of Elementary Gas Reactions*; Butterworth: London, 1980.
- (13) Gilbert, R. C.; Smith, S. C. *Theory of Unimolecular and Recombination Reactions*; Blackwells Scientific Publications: Oxford, 1990.
- (14) Sheldrick, G. S. *Structural Chemistry of Organic Silicon Compounds*. In *The Chemistry of Organic Silicon Compounds*; Rappoport, Z., Apeloig, Y., Eds.; Wiley: Chichester, 1989; Vol. 1, Chapter 3, p 227.
- (15) Legon, A. C. *Faraday Discuss.* **1994**, *97*, 19.
- (16) Robertson, S.; Wagner, A. F.; Wardlaw, D. M. *J. Chem. Phys.* **1995**, *103*, 2917; *J. Chem. Phys.* **2000**, *113*, 2648; *J. Phys. Chem. A* **2002**, *106*, 2598; *J. Chem. Phys.* **2002**, *117*, 593 and references cited therein.
- (17) Klippenstein, S. J. *Ber. Bunsen-Ges. Phys. Chem.* **1997**, *101*, 423 and references cited therein.
- (18) Smith, S. C. *J. Chem. Phys.* **1999**, *111*, 1830 and references cited therein.